Arab J Sci Eng (2014) 39:8517–8524
DOI 10.1007/s13369-014-1414-y

RESEARCH ARTICLE - CIVIL ENGINEERING

Effect of Rice Husk Ash on the Thaumasite Form of Sulfate Attack of Cement-Based Materials

Baoguo Ma · Yingbin Wang · Haobing Fu

Received: 15 January 2014 / Accepted: 31 August 2014 / Published online: 6 November 2014

Abstract The influence of rice husk ash (RHA) on the thaumasite formation of cement pastes containing limestone powder was investigated. The specimens which were cured in 2 % $MgSO_4$ solution were prepared with different ratios of coarse rice husk ash (CRHA) and fine rice husk ash (FRHA) to cement. The visual change of mortars was inspected monthly. Compressive strength, length and mass developments were examined as functions of time. The products of sulfate attack were examined by X-ray diffraction, Fourier transform infrared spectroscopy and Laser-Raman spectroscopy. The results showed that the degree of deterioration was retarded when cement was partially replaced by RHA. The use of FRHA showed better performance than those of the coarser ones. No obvious degeneration was observed in the mortar contains 20 % FRHA after 12 months of immersing in the $MgSO_4$ solution.

Keywords Sulfate attack · Thaumasite · Limestone · Rice husk ash (RHA)

B. Ma (✉) · Y. Wang · H. Fu
State Key Laboratory of Silicate Materials for Architectures,
Wuhan University of Technology,
Wuhan 430070, China
e-mail: 275331986@qq.com

الخلاصة

تم التحقيق في تأثير رماد قشر الأرز في تشكيل معدن سيليكات الثيومسايت من معاجين الإسمنت التي تحتوي على مسحوق الحجر الجيري. وتم إعداد العينات التي تم علاجها في 2٪ محلول كبريتات المغنيسيوم مع نسب مختلفة من رماد قشر الأرز الخشن ورماد قشر الأرز الناعم في الإسمنت. وتم فحص التغيير البصري من الهاونات شهريا. كما تم فحص قوة الضغط وتطورات الطول والكتلة كوظيفة من الوقت. وتم فحص النواتج من هجوم الكبريتات بوساطة حيود الأشعة السينية ، ومطيافية الأشعة تحت الحمراء المحولة بفوريه ومطيافية ليزر رامان. وأظهرت النتائج أن درجة التدهور قد تعطلت عندما تم استبدال الإسمنت جزئيا برماد قشر الأرز. وأظهر استخدام رماد قشر الأرز الناعم أداء أفضل من ذاك الخشن منه. لم يلاحظ أي تدهور واضح في الهاون الذي يحتوي على 20٪ رماد قشر أرز ناعم بعد 12 شهرا من الغمر في محلول كبريتات المغنيسيوم.

1 Introduction

As known to all, sulfate attack on cement-based material is a worldwide concern, because it may lead to expansion, mass loss and ultimately to disintegration [1]. This behavior is mainly due to the reaction of the hydration products of cement material with sulfate ions from the material or environment to gypsum, ettringite ($C_3A \cdot 3CaSO_4 \cdot 32H_2O$) and thaumasite ($CaSiO_3 \cdot CaCO_3 \cdot CaSO_4 \cdot 15H_2O$) [1,2]. The formation of thaumasite requires four primary risk factors: presence of carbonate, a source of sulfate, excess water and low temperature (<15 °C). The problem of thaumasite form of sulfate attack (TSA) was concerned during the past decades because of its prevalent in buried concrete [1,3]. TSA destroys the structure of calcium silicate hydrates (the main hydration product of cement paste) and leads to transformation of concrete into a mush from the surface inwards [3–9]. The optimum formation condition from cementitious materials, aggregates, additives and sulfate sources to thaumasite were clearly established [10–13].

Studies to date had been concentrated on the search of mortar or concrete mixes capable of resisting TSA, among which, the use of mineral admixtures had been a representative method for retarding the deterioration rate of TSA on cement-based materials in sulfate environments. Addition of mineral admixtures (fly ash, blast-furnace slag and rice husk ash (RHA)) not only modified the chemical properties of the cement-based materials by dilution of C_3A concentration and removal of CH through pozzolanic reaction, but also optimized the compactness of the mortar and concrete, and thus enhances the sulfate resistance of mixtures exposed to sulfate conditions [14,15].

The RHA obtained from rice husk under controlled burning conditions is a highly reactive pozzolanic material. Several investigators [16–19] reported the effectiveness of RHA in concrete performance. For example, concrete containing RHA exhibit higher compressive strength, low water absorption, low porosity and good resistance against the traditional sulfate attack. However, the influence of RHA on TSA in cement-based materials has not been reported. The objective of this work is to investigate the effect of RHA on the thaumasite formation in cement pastes containing limestone powder. Results of this work could be used to enhance the understanding of the durability of limestone–cement with RHA and could be referential in selection of materials subjected to sulfate environment.

2 Experimental Methodology

2.1 Raw Materials

The cement used in this work was Portland cement produced by YangFang Cement Company of Hubei province, in accordance with the Chinese standard GB 175 Type II (PII42.5). It has a mean grain size of 16.17 μm and specific surface area (Blaine fines) of 358 m^2/kg. The physical properties of cement are shown in Table 1. The limestone from Wuhan quarry was grinded using a ball mill for 30 min. The specific surface area of limestone powder is 390 m^2/kg. Rice husk from Hubei province was incinerated in a high-temperature furnace at 650 °C for 3 h. The incineration product was grinded using a ball mill for 15 and 180 min, respectively. The mean particle size of FRHA and CRHA was 10.66 and 25.35 μm, respectively. Table 2 presents the major constituents of each material. Chemical reagent of magnesium sulfate was used to prepare aggressive solution. SEM micrograph of the FRHA and CRHA is presented in Fig. 1. Figure 2 shows the particle size distribution of the three main materials.

Table 1 Physical properties of cement

Physical properties of cement	
Specific gravity	3.25
Initial setting time (min)	95
Final setting time (min)	215
Specific surface (m^2/Kg)	358
mineral composition (wt%)	
C_3S (%)	53.45
C_2S (%)	26.29
C_3A (%)	5.96
C_4AF (%)	8.27

2.2 Mix Design and Specimens Preparation

A series of cement pastes with water to binder mass ratio (W/B) of 0.485 and different RHA/binder ratios were prepared by a casting method. Table 3 shows the mix proportion of the samples. The test specimen is of a rectangular bar shape and two sizes of test specimens which were 40 mm × 40 mm × 160 mm and 25 mm × 25 mm × 285 mm were applied. Specimens having dimensions of 40 mm × 40 mm × 160 mm were used to measure mass and compressive strength, while 25 mm × 25 mm × 285 mm prisms were used to measure length change. All the specimens were demolded from the casting after 24 h and cured in water at 20 °C for 28 days. In order to study the compressive strength of mortars under TSA and to compare the results to normal condition, after 28 days of curing in water, all the mortars were stored in two different conditions: water at 5 ± 1 °C (control) and a 2 mass % magnesium sulfate solution at 5 ± 1 °C for 12 months. The solution was regularly changed monthly.

2.3 Methods

When the immersion ages of the specimens in solutions reached a certain point, for example, 0, 4, 8 and 12 months. A series of tests were performed on the specimens including investigations of the outward appearance, measurement of length and mass, as well as compressive strength. X-ray

Table 2 Chemical composition of raw materials (wt%)

Name	CaO	SiO_2	Al_2O_3	Fe_2O_3	MgO	SO_3	R_2O	f-CaO	IL
Cement	61.27	21.04	6.94	2.36	1.32	1.94	0.97	0.67	3.16
Limestone	51.35	51.35	5.63	1.82	0.56	–	–	–	40.41
RHA	1.24	88.65	0.51	0.86	0.29	–	3.54	–	–

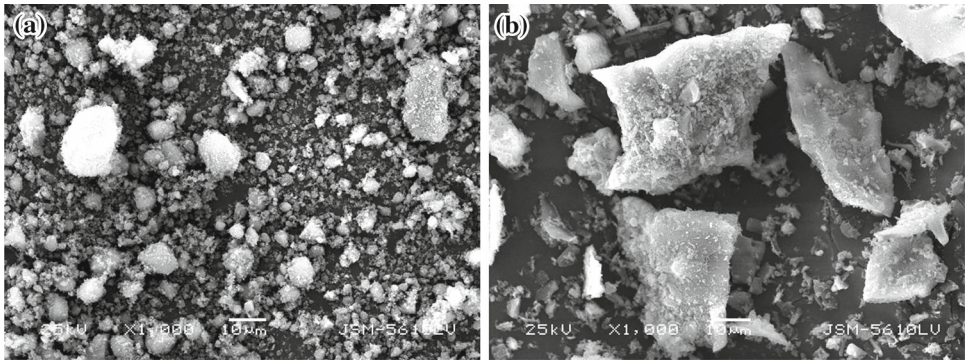

Fig. 1 SEM micrograph of (**a**) FRHA and (**b**) CRHA used in this study

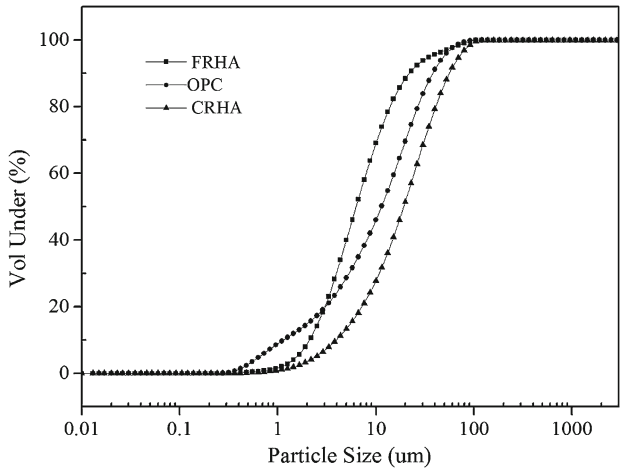

Fig. 2 Particle size distribution pattern of the different materials used in this study

Table 3 Mix proportion of the samples

Sample	Binder/kg				Sand/kg	Water/binder
	Cement	CRHA	FRHA	Limestone		
PC	408			72	1,320	0.485
CRHA5	384	24		72	1,320	0.485
CRHA10	360	48		72	1,320	0.485
CRHA20	312	96		72	1,320	0.485
FRHA5	384		24	72	1,320	0.485
FRHA10	360		48	72	1,320	0.485
FRHA20	312		96	72	1,320	0.485

diffraction (XRD), Fourier transform infrared (FTIR) spectroscopy and Laser-Raman spectroscopy were used to analyze the chemical characteristics of the specimens so as to distinguish the degradation products of the cement mortars after exposure to $MgSO_4$ solution. The samples used for micromorphology analysis were cut from the surface of the mortars. Pieces of the freshly cut samples were stored in isopropanol for at least 24 h. Samples were then grinded with isopropanol in a mortar and dried. Samples were finally passed through an 80 μm sieve.

X-ray diffraction patterns of the sample powder were collected on an XRD (Model D/MAX-IIIA, Japan) with CuKa radiation (35 kV, 30 mA) over an angular rotation from 5° to 60°.

FTIR (Model Nicolet 60 SXB FTIR, USA) was used. The range of wavenumber is between 400 and 4,000 cm^{-1}.

Raman spectroscopic measurement was carried out using a Renishaw Raman Microprobe (Type RM-1000).

3 Results

3.1 Visual Observation

Figure 3 shows the visual appearances of specimens after 12 months of immersion in 2 % $MgSO_4$ solution. This figure shows that the degree of the degeneration owing to $MgSO_4$ attack was reduced with the increasing RHA content. In the period of 12 months, no visual change was observed on the specimens during the first 3 months. The beginning of sample degeneration was first noted on the PC specimens after 4 months of exposure. Onset of deterioration found on sample surfaces was delayed for the mortars containing RHA. After 12 months of exposure, the PC mortars had the most severe degeneration. Soft white substance was formed on the surface, and part of the substance was precipitated on the container bottom due to its scaling. The strength of sample was much decreased. The surface of specimens CRHA5, CRHA10 and FRHA5 scaled off seriously. Corners of these specimens lost integrity, nevertheless the CRHA20 and FRHA10 specimens showed medium degeneration, even up to 12 months of exposure. Moreover, the FRHA20 test bar did not show any visible changes for up to 12 months.

Therefore, the visual inspection results showed that the RHA content and fineness have a resistance effect against the sulfate attack of cement mortars.

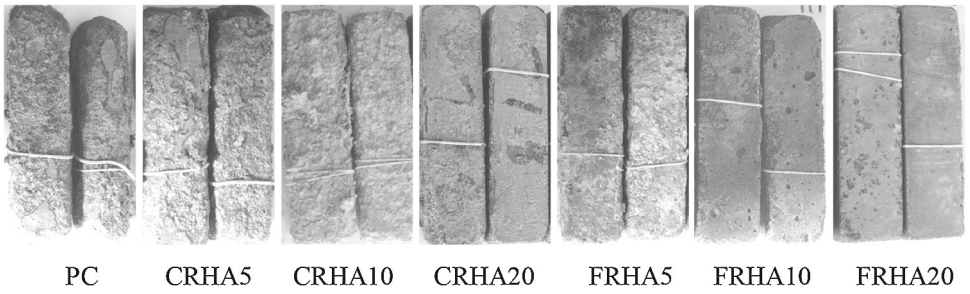

Fig. 3 Specimens cured for 12 months in 2 % $MgSO_4$ solution at 5 °C

Table 4 Compressive strength for the mortar exposed to sulfate and in water

Sample name	Compressive strength (MPa)								
	Water					Sulfate solution			
	28 days	90 days	180 days	270 days	360 days	90 days	180 days	270 days	360 days
PC	47.7	51.9	54.1	54.3	54.5	42.1	36.2	18.9	2.6
CRHA5	47.9	52.5	54.3	54.7	54.9	43.3	38.4	27.5	13.9
CRHA10	48.5	53.0	54.4	55.1	55.5	49.7	44.4	38.2	36.4
CRHA20	48.7	53.6	54.8	55.3	55.8	51.6	48.6	42.7	39.5
FRHA5	48.2	52.9	49.2	55.0	55.2	48.1	39.9	31.5	18.8
FRHA10	49.1	53.3	55.1	55.6	56.2	51.8	46.2	42.3	39.7
FRHA20	49.5	53.7	55.4	56.1	56.7	53.9	51.8	47.2	42.8

3.2 Compressive Strength

Table 4 presents the values of strength for the mortar bars immersed in water and those exposed to $MgSO_4$ solution. It is clear that the compressive strength values of samples exposed to $MgSO_4$ solution decreased in comparison with the samples immersed in water. The compressive strength of RHA-blended mortars in water even increased with the curing age compared with PC mortar. Table 4 also indicates that the fineness of RHA also affect the compressive strength of specimens. The mortars used FRHA seemed to gain higher compressive strength than those of the coarser ones.

Figure 4 presents the compressive strength relative loss (CSL) of the mortars after 12 months of immersion in $MgSO_4$ solution. The CSL is calculated on the basis of the strength of mortars immersed in sulfate solution after certain time, minus the initial strength of mortars before immersed in sulfate solution, divided by the initial strength, as expressed in the following equation:

$$\mathrm{CSL}(t) = [\mathrm{CS}_\alpha(t) - \mathrm{CS}_\alpha(0)] \times 100/\mathrm{CS}_\alpha(0) \quad (1)$$

where $\mathrm{CS}_\alpha(t)$ is the average strength of samples immersed in $MgSO_4$ solution, $\mathrm{CS}_\alpha(0)$ is the average strength of samples after 28 days curing in water, and α is the replacement level of RHA, as well as t is the time of exposure in $MgSO_4$ solution. As it can be deduced from Table 4 and Fig. 4 that mortars blended with RHA exhibited a better performance when immersed in aggressive solution, the CSL for the mortars

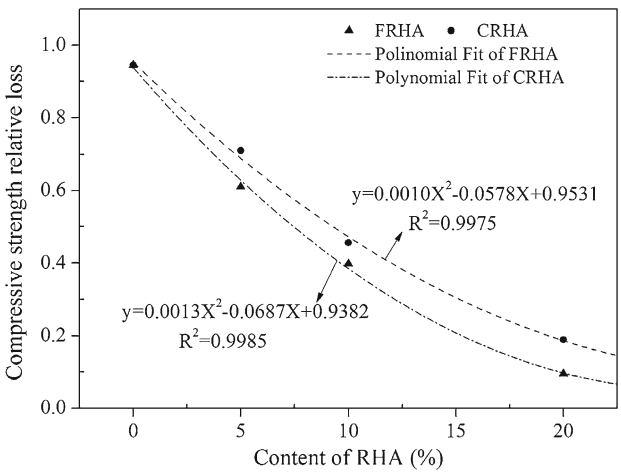

Fig. 4 Compressive strength evolution versus sulfate immersion time

containing RHA was decreased when the content of RHA is increased. Moreover, mortars containing RHA stored in sulfate always presented lower CSL value than PC mortar. The aforementioned phenomenon became more significant as curing time lapsed.

Figure 5 shows a relationship between compressive strength loss and replacement level of RHA. Regression analysis was applied in order to evaluate the correlation between the CSL and the content of RHA. Regression curves of a polynomial fit with correlation coefficients of 0.9975 and 0.9985 were drawn in the figure. The results indicated that strength loss decreased in a polynomial manner as RHA

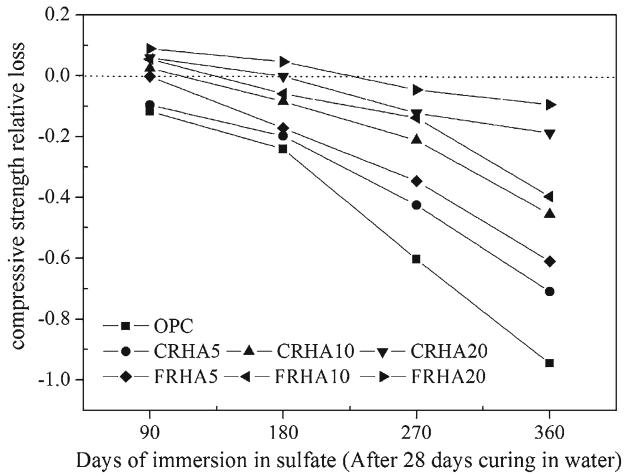

Fig. 5 Relationship between the strength loss of mortars and the cement replacement ratios after 12 months of immersion in sulfate solution

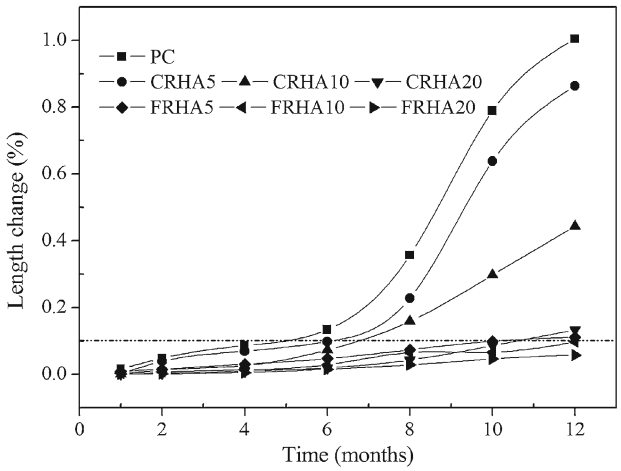

Fig. 6 Expansion of mortars exposed to $MgSO_4$ solution at 5 °C

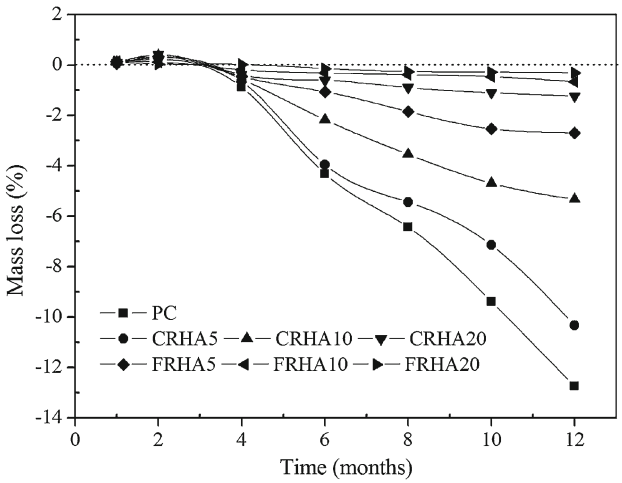

Fig. 7 Mass loss of mortar specimens exposed to $MgSO_4$ solution at 5 °C

content increased. The CSL of blank specimen was 94.5 %, and decreased to 61.0, 39.8 and 9.5 % in mortars with 5, 10 and 20 % FRHA, respectively. Figure 5 also indicates that the CSL decreases with finer RHA. The strength loss of CRHA20 was 18.9 %, and decreased to 9.5 % in mortar with 20 % FRHA. After application of 20 % RHA, the decrease in CSL seemed to reach a plateau.

3.3 Length Change

The effect of RHA on the length change (LC) of mortar specimens due to sulfate attack was studied. The length of specimens in different curing ages was tested, and the results were analyzed by using the following equation:

$$\mathrm{LC} = [L(t) - L(0)] \times 100/L(0) \tag{2}$$

where $L(t)$ is the average length of samples cured in $MgSO_4$ solution, $L(0)$ is the average length of specimens after 28 days of curing in water, and t is the time of exposure in $MgSO_4$ solution.

The LC of samples with time is presented in Fig. 6. The LC was found to be low in both the blank samples and the RHA samples within 6 months of exposure. However, after 12 months of exposure, the LC values of PC specimen increase dramatically while LC values of RHA specimens were much lower than that of PC specimens, most FRHA samples even below 0.100 %. For example, the *LC* for PC specimen was about 1.012 %, whereas specimens FRHA5, FRHA10 and FRHA20 showed expansions of 0.113, 0.097 and 0.058 %, respectively. These results indicated that specimens containing RHA showed better performance than control mortar (PC). Besides, the expansion was also influenced by the RHA fineness. The expansion of mortar CRHA20 was 0.132 %, while the expansion of sample containing 20 % of FRHA was 0.058 %, which indicated that the use of FRHA had even lower expansion than those of the coarser ones.

3.4 Mass Change

Figure 7 presents the mass change of mortars immersed in $MgSO_4$ solution. As for cement-based materials, the mass loss was mainly due to a reaction of the hydration products of cement paste with sulfate ions to sulfate-bearing substances, which can lead to serious degradation. The mass of specimens in different curing ages was tested, and the results were analyzed by using the following equation:

$$\mathrm{MC} = [M(t) - M(0)] \times 100/M(0) \tag{3}$$

where $M(t)$ is the average mass of samples cured in $MgSO_4$ solution, $M(0)$ is the average mass of specimens after 28 days

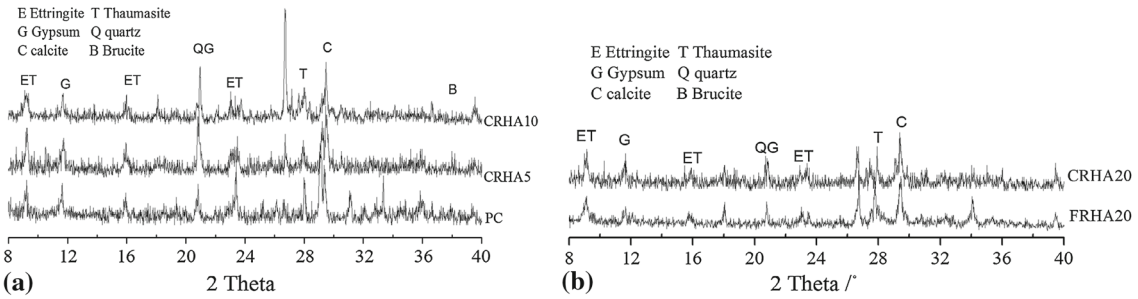

Fig. 8 XRD patterns of the mortar prisms after 1 year exposure to $MgSO_4$. **a** CRHA content. **b** CRHA20 and FRHA20

of curing in water, and t is the time of exposure in $MgSO_4$ solution.

From this figure, it is clear that the PC specimen has the largest mass loss (12.74 %) after 12 months of exposure. It is obvious that mortars with higher contents of RHA exhibited better stability. For example, the mass loss of specimens CRHA20 and FRHA20 after 12 months of exposure was 4.24 and 0.31 %, respectively. It can also be seen that the use of FRHA had lower mass loss than those of the coarser ones. The results of mass change test are in accordance with the results from the compressive strength test and length change test.

3.5 Mineralogy Analysis

The XRD patterns of the surface of mortar bars after 12 months of immersion in sulfate solution are shown in Fig. 8. It is indicated that gypsum (at 11.5°), brucite ($Mg(OH)_2$, at 18.5° and 38.0°), thaumasite (at 9.2°) and/or ettringite (at 9.1°) are the major crystalline phases present in the tested samples. However, no detectable $Ca(OH)_2$ was found in the PC mortar.

Thaumasite belongs to the ettringite-like mineral group, which has a similar XRD pattern with ettringite due to its similarity in crystallographic structure and morphology with ettringite, so thaumasite and ettringite are hardly separated in their XRD pattern [20]. Moreover, possible formation of thaumasite–ettringite solid solutions makes the identification more complex. Therefore, the products and types of sulfate attack in the samples could not be confirmed by the XRD patterns, and it is recommended by this work that further investigation should be conducted by suitable characterization techniques to distinguish ettringite and thaumasite in the future TSA studies.

Figure 9 presents the FTIR spectra of the mortar specimens with different replacement levels of RHA after immersion in $MgSO_4$ solution for 12 months. The absorption bands were identified by reference to previously published IR data on ettringite and thaumasite as showed in Table 5 [21,22]. The obvious peaks at about 499 and 670 cm^{-1} of all the specimens are assigned to SiO_6 group, and this state of Si–O

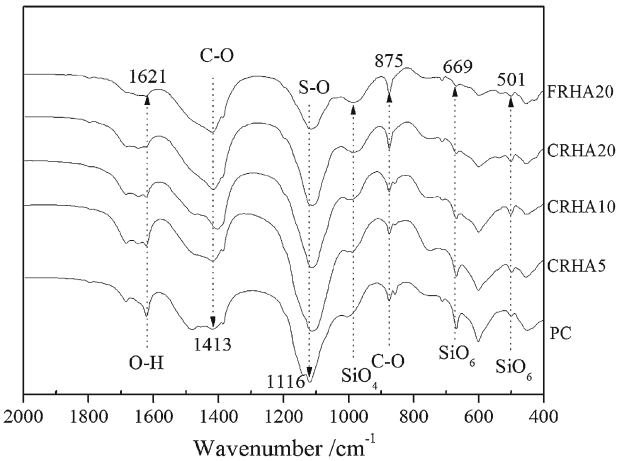

Fig. 9 FTIR spectra of specimens

Table 5 Wavenumber of important absorption bends

Wavenumber/cm^{-1}	Assignment
1,680	O–H bend
1,400	C–O stretching (CO_3^{2-})
1,100	S–O stretching (SO_4^{2-})
940/920	SiO_4
875	C–O bend (CO_3^{2-})
750	SiO_6 stretching
500	SiO_6 bending

indicates the existence of thaumasite. The peaks at 851 cm^{-1} were assigned to the presence of AlO_6 group; the medium strong peak at 875 cm^{-1} is ascribed to C–O bending vibration of CO_3^{2-} group, and the broad band at about 1,413 cm^{-1} is attributed to C-O stretching vibration of CO_3^{2-} group. A strong peak at 1,116 cm^{-1} associated with SO_4^{2-} group (S–O) indicates the formation of massive sulfate-bearing substances like ettringite or gypsum. Consequently, it can be confirmed that the deteriorated samples contained mainly thaumasite, ettringite and gypsum in specimens PC, CRHA5 and CRHA10, but there is little thaumasite in specimens CRHA20 and FRHA20.

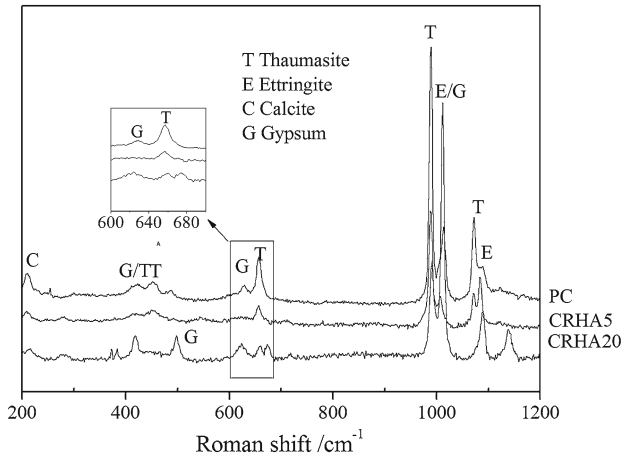

Fig. 10 Raman spectra of specimens

Table 6 Characteristic peak value of various matters in Raman spectra

Matter	Major peaks location/cm^{-1}	Minor peaks location/cm^{-1}
Thaumasite	658, 990, 1,076	417, 453, 479
Ettringite	988, 1,088	449, 548, 617
Calcite	1,086	713, 285
Gypsum	1,009	417, 496, 621, 673, 1,137

Figure 10 shows the Raman spectra for the deteriorated samples (PC, CRHA5 and CRHA20). The characteristic peaks were identified via the comparison with previously published data (Table 6) [4,23]. The intensive peaks at 658, 990 and 1,076 cm^{-1} were due to silicate, sulfate and carbonate groups, respectively. In addition, the peaks at 417 and 496 cm^{-1} that were assigned to gypsum vibration are found in Fig. 10, which reconfirmed the presence of thaumasite, ettringite, gypsum and calcite in all specimens. Moreover, the samples in order of peak intensity from high to low are PC, CRHA5 and CRHA20. The Raman spectra results further reconfirmed the results mentioned in FTIR results as discussed above.

4 Discussion

All experimental results obtained from this study confirm that the incorporation of RHA exhibited superior resistance to TSA. The results of mechanical properties indicated that samples contained RHA presented relatively high values compared with PC specimens. This improvement accompanied with low expansion and mass loss values of mortars. In addition, microstructure analysis showed that there was a significant reduction of sulfate products for specimens contained RHA when compared to PC specimen. This fact can be attributed to the physical and chemical effects of RHA.

Specifically, the incorporation of RHA could fill in the pore space within the mortar leading to a more compact structure. This may imply, to a degree, the low permeability of RHA specimens. In other words, the lower permeability of RHA samples makes the ingress of sulfate ion from solution more difficult. Investigations had revealed that the permeability of structure is closely related to sulfate attack [24,25]. From the results of macroscopic properties, it was evident that the degradation of PC specimen was more obviously than that of RHA specimens.

In addition to the permeability, the reduction in soluble calcium hydroxide due to the pozzolanic reaction is also beneficial in reducing the quantity of gypsum and ettringite (caused by sulfate attack). Besides, RHA can react with calcium hydroxide to form secondary C–S–H; this kind of hydration product of pozzolanic reaction would increase packing density of concrete and mortar structure through pore-size refinement [26]. Secondary C–S–H has a low CaO/SiO_2 ratio, and the structural is different from the C–S–H of cement paste. It contains relatively less Ca in its structure, and thus, RHA specimens expected to be more durable than PC specimen in a sulfate condition [27]. It should be noted that the incorporation of RHA could effectively improve the cement-aggregate bond at interfaces in the internal structure of mortar and concrete [28].

Moreover, the replacement of Portland cement by RHA led to the dilution of tricalcium aluminate. The formation mechanism for thaumasite is the direct reactions among C–S–H and appropriate portion of carbonate, sulfate, Ca^{2+} ions and excess water, which would lead to the disintegration of C–S–H and the formation of no-strength-bearing substance thaumasite. Meanwhile, the thaumasite formation would be accelerated due to an appropriate amount of aluminum-bearing phase [29,30]. Therefore, the degree of deterioration was retarded when cement was partially replaced by RHA.

The deterioration degree of the specimens was affected not only by the content of RHA, but also by the fineness of RHA. This is because the RHA with higher surface areas and finer particle size could more effectively fill in the pore space within the mortar; moreover, the silica of FRHA could be dissolved relative easily and react with portlandite to form more C–S–H which would finally lead to a more compact structure with higher density [31].

5 Conclusions

The results in this study confirmed a strong effect of RHA on the degree of deterioration of cement-based material. Through microcosmic and macroscopic tests, the deterioration was serious in the PC specimens with 94.5 % CLS and massive sulfate-bearing substances, while it was relatively slight in RHA-blended specimens. The degree of de-

terioration of RHA-blended specimens was inhibited with an increase in the content of RHA. For example, the CLS of FRHA5 specimen was 61.0 %, while the CLS of sample containing 20 % of FRHA was 13.5 %. In addition to the RHA content, the fineness of RHA has a remarkable effect on the TSA resistance of mortar specimens. Specimens with FRHA showed higher TSA resistance than mortars contained CRHA. No obvious degeneration was presented in the mortars contained 20 % FRHA after 12 months immersion in $MgSO_4$ solution at 5 °C.

Acknowledgments This work is funded by National Natural Science Foundation of China (Nos. 51178363 and 51378408).

References

1. Clark, L.: The thaumasite form of sulfate attack: risks, diagnosis, remedial works and guidance on new construction. Report of the Thaumasite Expert Group. Department of the Environment, Transport and the Regions (1999)
2. Irassar, E.: Sulfate attack on cementitious materials containing limestone filler—a review. Cem. Concr. Res. **39**(3), 241–254 (2009)
3. Ma, B. et al.: Thaumasite formation in a tunnel of Bapanxia Dam in Western China. Cem. Concr. Res. **36**(4), 716–722 (2006)
4. Skaropoulou, A.; Kakali, G.; Tsivilis, S.: A study on thaumasite form of sulfate attack (TSA) using XRD, TG and SEM. J. Thermal Anal. Calorim. **84**(1), 135–139 (2006)
5. Hartshorn, S.; Sharp, J.; Swamy, R.: Thaumasite formation in Portland-limestone cement pastes. Cem. Concr. Res. **29**(8), 1331–1340 (1999)
6. Gaze, M.; Crammond, N.: The formation of thaumasite in a cement: lime: sand mortar exposed to cold magnesium and potassium sulfate solutions. Cem. Concr. Compos. **22**(3), 209–222 (2000)
7. Hartshorn, S.; Sharp, J.; Swamy, R.: The thaumasite form of sulfate attack in Portland-limestone cement mortars stored in magnesium sulfate solution. Cem. Concr. Compos. **24**(3), 351–359 (2002)
8. Barker, A.; Hobbs, D.: Performance of Portland limestone cements in mortar prisms immersed in sulfate solutions at 5 C. Cem. Concr. Compos. **21**(2), 129–137 (1999)
9. Bellmann, F.; Stark, J.: Prevention of thaumasite formation in concrete exposed to sulphate attack. Cem. Concr. Res. **37**(8), 1215–1222 (2007)
10. Smallwood, I.; Wild, S.; Morgan, E.: The resistance of metakaolin (MK)–Portland cement (PC) concrete to the thaumasite-type of sulfate attack (TSA)—Programme of research and preliminary results. Cem. Concr. Compos. **25**(8), 931–938 (2003)
11. Tsivilis, S. et al.: Use of mineral admixtures to prevent thaumasite formation in limestone cement mortar. Cem. Concr. Compos. **25**(8), 969–976 (2003)
12. Skaropoulou, A.; Kakali, G.; Tsivilis, S.: Thaumasite form of sulfate attack in limestone cement concrete: the effect of cement composition, sand type and exposure temperature. Constr. Build. Mater. **36**, 527–533 (2012)
13. Kakali, G. et al.: Parameters affecting thaumasite formation in limestone cement mortar. Cem. Concr. Compos. **25**(8), 977–981 (2003)
14. Baghabra, O.S.; Al-Amoudi, M.M.; Saadi, M.M.: Effect of magnesium sulfate and sodium sulfate on the durability performance of plain and blended cements. ACI Mater. J. **92**(1), 15–24 (1995)
15. Veiga, K.; Gastaldini, A.: Sulfate attack on a white Portland cement with activated slag. Constr. Build. Mater. **34**, 494–503 (2012)
16. Sousa Coutinho, J.: The combined benefits of CPF and RHA in improving the durability of concrete structures. Cem. Concr. Compos. **25**(1), 51–59 (2003)
17. Saraswathy, V.; Song, H.-W.: Corrosion performance of rice husk ash blended concrete. Constr. Build. Mater. **21**(8), 1779–1784 (2007)
18. Ramadhansyah, P. et al.: Properties of concrete containing rice husk ash under sodium chloride subjected to wetting and drying. Proc. Eng. **50**, 305–313 (2012)
19. Kathirvel, P. et al.: Strength and durability properties of quaternary cement concrete made with fly ash, rice husk ash and limestone powder. Arab. J. Sci. Eng. **38**(3), 589–598 (2013)
20. Ma, B. et al.: Microscopic structure and growth mechanism of the corrosion products including thaumasite. J. Chin. Ceram. Soc. **34**(12), 1503–1507 (2006)
21. Bensted, J.; Varma, S.P.: Studies of thaumasite—part II. Silic. Ind. **39**(1), 11–19 (1974)
22. Hughes, T.L. et al.: Determining cement composition by Fourier transform infrared spectroscopy. Adv. Cem. Based Mater. **2**(3), 91–104 (1995)
23. Sahu, S.; Exline, D.L.; Nelson, M.P.: Identification of thaumasite in concrete by Raman chemical imaging. Cem. Concr. Compos. **24**(3), 347–350 (2002)
24. Mehta, P.K.: Durability of concrete in marine environment—a review. ACI Spec. Publ. **65**, 1–20 (1980)
25. Roy, D.: Hydration, structure, and properties of blast furnace slag cements, mortars, and concrete. ACI J. Proc. (1982)
26. Mehta, P.K.; Monteiro, P.J.: Concrete: Microstructure, Properties, and Materials, vol. 3, pp. 265–268. McGraw-Hill, New York (2006)
27. Bakharev, T.; Sanjayan, J.; Cheng, Y.-B.: Sulfate attack on alkali-activated slag concrete. Cem. Concr. Res. **32**(2), 211–216 (2002)
28. Giaccio, G.; de Sensale, G.R.; Zerbino, R.: Failure mechanism of normal and high-strength concrete with rice-husk ash. Cem. Concr. Compos. **29**(7), 566–574 (2007)
29. Köhler, S.; Heinz, D.; Urbonas, L.: Effect of ettringite on thaumasite formation. Cem. Concr. Res. **36**(4), 697–706 (2006)
30. Vuk, T.; Gabrovšek, R.; Kaučič, V.: The influence of mineral admixtures on sulfate resistance of limestone cement pastes aged in cold $MgSO_4$ solution. Cem. Concr. Res. **32**(6), 943–948 (2002)
31. Nazari, A.; Bagheri, A.; Riahi, S.: Properties of geopolymer with seeded fly ash and rice husk bark ash. Mater. Sci. Eng. A **528**(24), 7395–7401 (2011)